NMDA receptors in preBötzinger complex neurons can drive respiratory rhythm independent of AMPA receptors

Consuelo Morgado-Valle and Jack L. Feldman

Systems Neurobiology Laboratory, Department of Neurobiology, David Geffen School of Medicine at UCLA, University of California Los Angeles, Box 951763, Los Angeles, CA 90095-1763, USA

The role of AMPA receptors (AMPARs) in generation and propagation of respiratory rhythm is well documented both *in vivo* and *in vitro*, whereas the functional significance of NMDA receptors (NMDARs) in preBötzinger complex (preBötC) neurons has not been explored. Here we examined the interactions between AMPARs and NMDARs during spontaneous respiratory rhythm generation in slices from neonatal rats *in vitro*. We tested the hypothesis that activation of NMDARs can drive respiratory rhythm in the absence of other excitatory drives. Blockade of NMDARs with dizocilpine hydrogen maleate (MK-801, 20 μM) had a negligible effect on respiratory rhythm and pattern under standard conditions *in vitro*, whereas blockade of AMPARs with NBQX (0.5 μM) completely abolished respiratory activity. Removal of extracellular Mg^{2+} to relieve the voltage-dependent block of NMDARs maintained respiratory rhythm without a significant effect on period, even in the presence of high NBQX concentrations ($\leq 100\ \mu$M). Removal of Mg^{2+} increased inspiratory-modulated inward current peak (I_I) and charge (Q_I) in preBötC neurons voltage-clamped at -60 mV by 245% and 309%, respectively, with respect to basal values. We conclude that the normal AMPAR-mediated postsynaptic current underlying respiratory drive can be replaced by NMDAR-mediated postsynaptic current when the voltage-dependent Mg^{2+} block is removed. Under this condition, respiratory-related frequency is unaffected by changes in I_I, suggesting that the two can be independently regulated.

Glutamate is the major fast excitatory neurotransmitter underlying respiratory rhythm generation. AMPAR and NMDAR antagonist microinjections *in vivo* in adult mammals suggest a synergistic role of these receptors in the transmission of inspiratory drive to motoneurons. Microinjection of either the AMPAR antagonist 2,3-dihydroxy-6-nitro-7-sulfamoyl-benzo(f)quinoxalline (NBQX) or the NMDAR antagonist D(−)-2-amino-7-phosphonoheptanoic acid (AP-7) into the phrenic motor nucleus decreases the amplitude of phrenic nerve bursts in rats. However, simultaneous blockade of both receptors decreases the amplitude in a synergistic way (Chitravanshi & Sapru, 1996). Although NMDARs and AMPARs coexist in respiratory rhythm generation-related areas, only AMPAR-mediated transmission is essential for rhythm generation and propagation both *in vivo* in adult rat (Connelly *et al.* 1992; Chitravanshi & Sapru, 1996) and cat (Anderson & Speck, 1999), and *in vitro* in neonatal rat (Greer *et al.* 1991; Funk *et al.* 1993). Moreover, *in vitro* preparations from neonatal mutant mice lacking the NMDAR1 subunit generate a rhythm

that is indistinguishable from that obtained from neonatal wild-type mice, demonstrating that NMDARs are not essential for respiratory rhythm generation or drive transmission in the neonate (Funk *et al.* 1997). However, this does not mean that NMDARs are superfluous. In *in vitro* preparations generating respiratory rhythm, while the NMDAR antagonist dizocilpine hydrogen maleate (MK-801) does not perturb spontaneous respiratory burst frequency, bath application of NMDA produces a dose-dependent increase in respiratory frequency (Greer *et al.* 1991; Funk *et al.* 1993). Furthermore, *in vivo*, anaesthetized cats breathe normally after systemic administration of MK-801, but subsequent vagotomy produces apneusis (Foutz *et al.* 1988, 1989; Feldman *et al.* 1992).

Complicating our understanding of the contribution of NMDARs to rhythm generation is its voltage dependence: at resting membrane potentials (≤ -60 mV), currents through activated NMDARs are substantially attenuated by Mg^{2+} in physiological concentrations (0.8–1.2 mM), but as the membrane depolarizes, the

Mg^{2+} blockade is relieved. Here we examined the effects of removing NMDAR blockade during perturbations of AMPAR-mediated transmission on rhythmic activity of preBötC neurons and integrated hypoglossal nerve ($\int$XIIn) activity in a neonatal rat medullary slice preparation. We found that under conditions where the voltage-dependent Mg^{2+} block of NMDARs is relieved, substantial currents can pass through NMDARs sufficient to drive the rhythm when AMPARs are blocked. Moreover, even though in the absence of Mg^{2+} there is a 4-fold increase on preBötC neuron inspiratory-modulated inward current peak (I_I), respiratory frequency remained unaffected. We show that the NMDAR can substitute, after removing its voltage-dependent block due to Mg^{2+}, for the AMPAR glutamatergic transmission normally underlying respiratory pattern generation in the *in vitro* slice preparation.

Methods

Slice preparation

Experiments were performed on neonatal rat transverse brainstem slices that generate respiratory-related motor output (Smith *et al.* 1991). The Office for the Protection of Research Subjects, University of California Research Committee approved all protocols. Briefly, neonatal rats (0–3 days old) were anaesthetized with isoflurane, decerebrated and the neuroaxis was isolated. The cerebellum was removed and the brainstem sectioned serially in the transverse plane using a VT-1000 Vibratome (Vibratome, St Louis, MO, USA) until neuroanatomical landmarks, i.e. nucleus ambiguus and inferior olive, were visible. A transverse slice (550 μm) containing the preBötC was cut. The dissection was performed in an artificial cerebrospinal fluid (ACSF) containing (mM): 128 NaCl, 3 KCl, 1.5 $CaCl_2$, 1 $MgSO_4$, 23.5 $NaHCO_3$, 0.5 NaH_2PO_4 and 30 glucose, bubbled with 95% O_2–5% CO_2 at 27°C. The slice was transferred to a 1 ml recording chamber and anchored using a platinum frame and a grid of nylon fibres. The chamber was mounted to a fixed-stage microscope and perfused with ACSF (6 ml min^{-1}).

Rhythmic respiratory-related motor output was recorded from the XIIn using fire-polished glass suction electrodes and a differential amplifier. To obtain a robust and stable rhythm, ACSF K^+ concentration was elevated to 9 mM and slices were perfused for 30 min before any experimental manipulation. XIIn activity was amplified, bandpass filtered (0.3–1 kHz), rectified and integrated ($\tau = 20$ ms; $\int$XIIn). For 0 mM Mg^{2+} ACSF, 1 mM $MgSO_4$ was removed. Only one experiment was performed per neuron per slice.

Drugs, obtained from Sigma Chemical Co. (St Louis, MO, USA), were bath applied at the following concentrations: 1 μM tetrodotoxin (TTX), 5 μM bicuculline, 2 μM strychnine, 0.001–100 μM NBQX in a cumulative way, 20 μM MK-801. We used 20 μM MK-801 to specifically block NMDA receptors and avoid non-specific effects (Rothman, 1988; Wooltorton & Mathie, 1995). DL-Threo-β-benzyloxyaspartate (TBOA, 100 μM) was obtained from Tocris (Ellisville, MO, USA).

Patch-clamp recording

Inspiratory neurons from preBötC were visualized using infrared-enhanced differential interference contrast videomicroscopy. Whole-cell patch-clamp recordings were performed using an Axopatch 200A amplifier (Axon Instruments) for voltage-clamp and current-clamp experiments. Electrodes were pulled from borosilicate glass (o.d., 1.5 mm; i.d., 0.86 mm) on a horizontal puller. Electrodes were filled with solution containing (mM): 140 potassium gluconate, 5 NaCl, 10 Hepes, 0.1 EGTA, 2 Mg-ATP, and 0.3 Na_3-GTP (pH 7.3). Input resistance (R_{in}) was determined from the current–voltage relationship generated by slow voltage-ramp commands ($\sim$10 mV s^{-1}) in the linear region negative to -50 mV. Cell capacitance (C_M) was determined from the integral of the transient capacitive current (I_C, leak subtracted) evoked by 15 ms hyperpolarizing voltage steps (ΔV_M), using the formula $C_M = \int I_C / \Delta V_M$. Series resistance ($R_s$) was then calculated from the decay-time constant (τ) of I_C since $\tau \sim R_S C_M$ in voltage-clamp, where τ is the estimated exponential I_C decay time. An acceptable voltage-clamp requires $R_{in} \geq 10 \times R_S$. Neurons failing to meet this criterion were discarded. R_S averaged 19.2 ± 0.9 MΩ ($n = 25$) and was compensated to 11.0 ± 0.6 MΩ via analog feedback. R_S compensation was applied without whole-cell capacitance compensation in order to continuously monitor τ and ensure stationary voltage-clamp conditions.

Electrophysiological signals were acquired digitally at 4–20 kHz using pCLAMP software and a Digidata 1320 AD/DA board (Axon Instruments) after low-pass filtering. Igor Pro (Wave Metrics, Inc., OR, USA), Chart (www.ADInstruments.com) and Microsoft Excel were used for data analyses.

Inspiratory-modulated inward current peak (I_I) was collected from cycles obtained during 3 min recording of steady state activity and averaged. Steady state for each experimental condition was considered after 10 min. Values were normalized against control. Synaptic charge (Q_I) was computed from the integral of the envelope of I_I measured at -60 mV.

Excitatory postsynaptic currents were elicited by 100 μM glutamate (I_{Glu}) applied locally with a pressure ejection system (Picospritzer II, General Valve Corp, Fairfield, NJ, USA). Inspiratory neurons were synaptically isolated by 1 μM TTX, and 5 μM bicuculline and 2 μM strychnine to abolish the contribution of spontaneous currents

mediated by activation of $GABA_A$ and glycine receptors. Pressure ejection pipettes were standard unpolished patch-electrodes positioned at a distance of 30–$40\ \mu m$ from the recorded neuron. The pressure applied ranged between 10 and 20 p.s.i. and the time for each application was 5 ms.

Results are expressed as means $\pm$ s.e.m. ANOVA and Student's *t* test were used when appropriate.

Results

AMPARs are obligatory for respiratory rhythm generation; NMDARs are not necessary

Bath application of NBQX at increasing concentrations: (i) decreased $\int$XIIn peak amplitude in a dose-dependent manner ($EC_{50} = 0.07\ \mu M$, $n = 4$, Fig. 1A); I_I peak recorded in voltage-clamp at $-60\ mV$ ($EC_{50} = 0.02\ \mu M$, $n = 4$, Fig. 5A), and; (ii) increased the period ($EC_{50} = 0.13\ \mu M$, Fig. 1A). Concentrations of NBQX between 0.1 and 0.5 μM

eliminated inspiratory currents and hence XIIn activity (Fig. 1B).

Bath application of MK-801 ($20\ \mu M$) did not significantly affect $\int$XIIn peak amplitude (Fig. 1A, $n = 13$), the I_I peak and synaptic charge (Q_I) in voltage-clamp at $-60\ mV$ ($n = 9$, Figs 1C and 2A) or the mean period (from 7.4 ± 1.2 s in control conditions to 8.5 ± 1.1 s, $n = 13$, Fig. 1A).

NMDARs contribute to I_I when Mg^{2+} blockade is removed by depolarization

We questioned whether AMPARs dominate respiratory drive under control conditions due to suppression of NMDAR currents resulting from the latter's voltage-dependent Mg^{2+} block. In order to eliminate this block, we voltage-clamped preBötC neurons at $+40\ mV$ (due to a reversal potential of $\sim0\ mV$, at this voltage I_I is outward). Subsequent bath application of MK-801 decreased the I_I peak by 25% ($P < 0.05$,
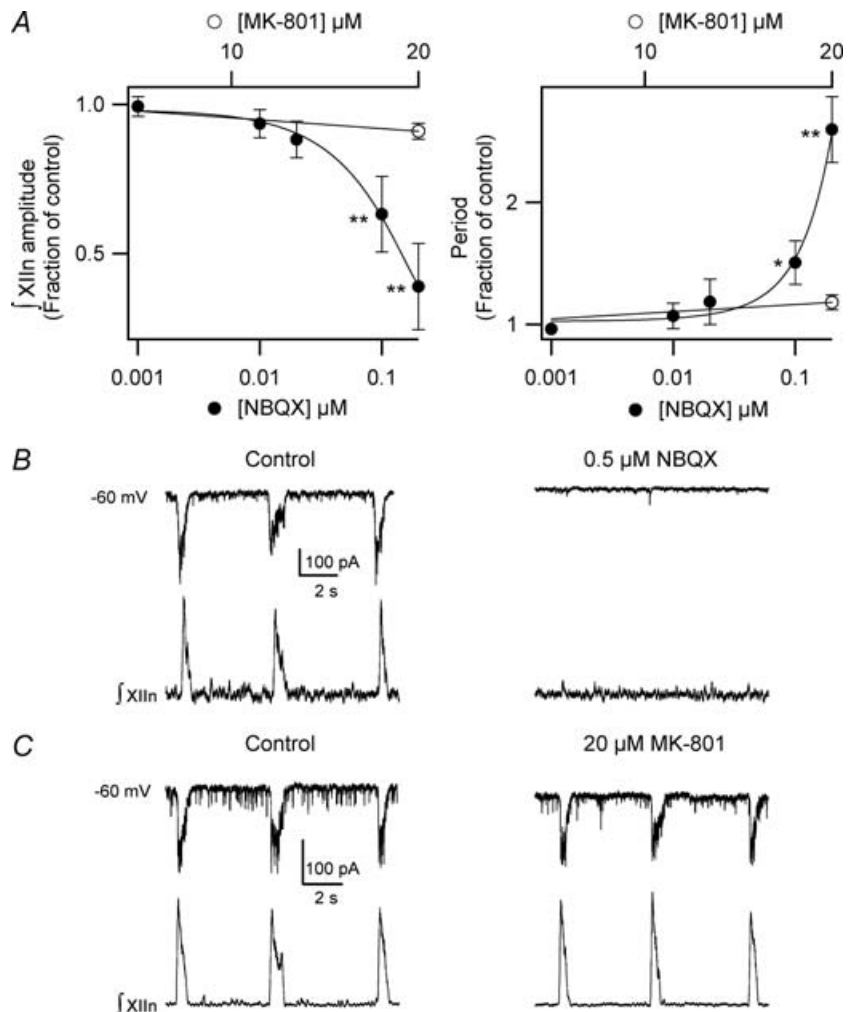

Figure 1. AMPARs are obligatory for respiratory rhythm generation; NMDARs are not necessary
A, antagonism of AMPARs with NBQX produced a dose-dependent decrease of the $\int$XIIn amplitude ($EC_{50} = 0.07\ \mu M$) and an increase in period ($EC_{50} = 0.13\ \mu M$). Antagonism of NMDAR with MK-801, did not significantly affect $\int$XIIn amplitude or period. *B*, representative I_I from a preBötC neuron and $\int$XIIn discharge recorded from a neonate rat rhythmic slice in standard conditions. Bath application of 0.1–0.5 μM NBQX completely abolished respiratory activity at the system and single unit levels. *C*, bath application of 20 μM MK-801 alone did not significantly affect respiratory activity at the system and single unit levels. (*$P < 0.05$; **$P < 0.01$.)

$n = 5$, Fig. 2B) and decreased Q_I by 56% with respect to basal conditions ($P < 0.001$, Fig. 2B). Thus when the voltage-dependent Mg^{2+} block is removed, a substantial NMDAR-component contributes to I_I.

Inhibition of glutamate uptake unmasks a substantial population of NMDARs in preBötC neurons

The current elicited by local pressure ejection of 100 μM glutamate in synaptically isolated (with bath-applied TTX)
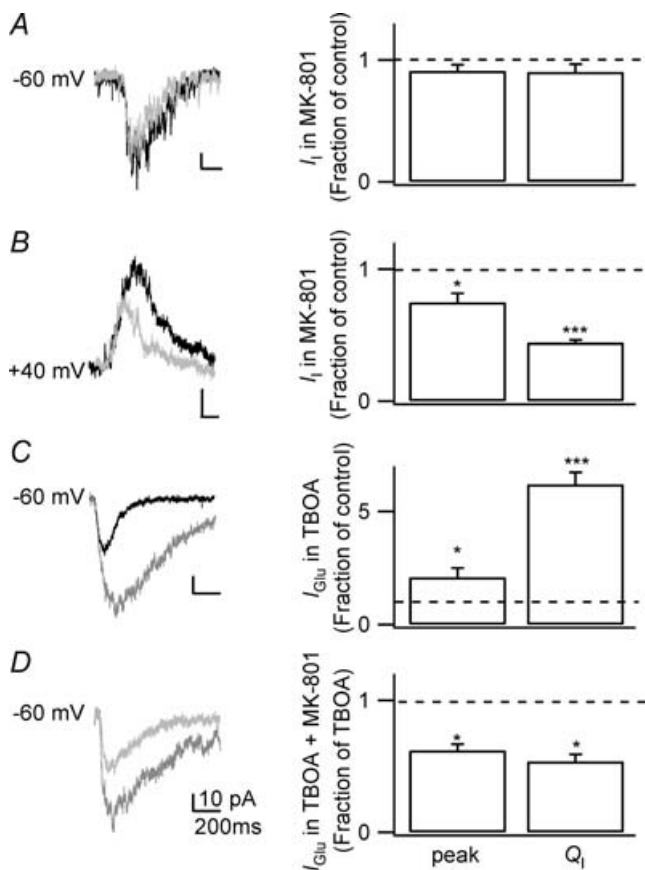
Figure 2. NMDARs are present but not passing current in preBötC neurons in standard *in vitro* conditions
A, black trace: I_I from a preBötC neuron voltage-clamped at -60 mV. Gray trace: I_I from same neuron in the presence of 20 μM MK-801. MK-801 did not significantly affect I_I amplitude. B, black trace: I_I from a preBötC neuron voltage-clamped at $+40$ mV. Note at this voltage I_I is outward. Dark grey trace: I_I from same neuron in the presence of 20 μM MK-801. Relief of voltage-dependent Mg^{2+} blockade unmasked a large component of NMDAR contributing to I_I. C, black trace: I_{Glu} elicited by local pressure ejection of 100 μM glutamate in a synaptically isolated preBötC neuron voltage clamped at -60 mV. Gray trace: I_{Glu} elicited with same parameters but in the presence of 100 μM TBOA. Glutamate uptake blockade significantly increased I_I peak and area. D, dark grey trace: I_{Glu} in 100 μM TBOA. Light grey trace: I_{Glu} in 100 μM TBOA and 20 μM MK-801. In the presence of TBOA, a large fraction of I_{Glu} is NMDAR mediated. In this and subsequent figures, data were normalized against control (control = 1, dashed line), except in D in which data were normalized against values in TBOA. (*$P < 0.05$; **$P < 0.01$; ***$P < 0.001$.)

preBötC neurons (I_{Glu}) was measured in voltage clamp at -60 mV. The non-transportable glutamate uptake inhibitor TBOA (100 μM) was then bath-applied. TBOA increased I_{Glu} by 110% ($P < 0.05$) and increased Q_{Glu} by 520% ($P < 0.001$) ($n = 4$, Fig. 2C). To measure the contribution of NMDAR-mediated current to this increase we added MK-801 to the bath. MK-801 reduced both I_{Glu} and Q_{Glu} by 40% ($P < 0.05$) and 45% ($P < 0.05$), respectively, with respect to I_{Glu} in the presence of TBOA alone ($n = 4$, Fig. 2D).

Endogenous NMDAR activation affects ∫XIIn amplitude and area, I_I and Q_I, but not period

In order to investigate the effects of endogenous NMDAR activation at the network level, i.e. XIIn motor output, we removed the NMDAR Mg^{2+} blockade. Thus, after recording basal rhythmic activity, control ACSF (containing 1 mM Mg^{2+}) was replaced by an ACSF lacking Mg^{2+}, i.e. 0 mM Mg^{2+}. Under control conditions, the period of ∫XIIn was 6.3 ± 1.2 s ($n = 4$); 0 mM Mg^{2+} ACSF did not significantly affect the period (5.5 ± 0.7 s, $n = 4$) but significantly increased ∫XIIn amplitude and area 28% ($P < 0.05$) and 43% ($P < 0.05$), respectively (Fig. 3A and B, $n = 4$). Subsequent bath application of MK-801 (during 0 mM Mg^{2+} ACSF perfusion) abolished the effects induced by 0 mM Mg^{2+} ACSF and brought ∫XIIn amplitude, area and period values back to control levels (Fig. 3B).

Compared to control ACSF, 0 mM Mg^{2+} ACSF significantly increased I_I peak and Q_I in preBötC neurons voltage-clamped at -60 mV by 245% ($P < 0.01$, $n = 3$, Fig. 3C) and 309% ($P < 0.01$), respectively.

NMDARs drive the respiratory rhythm in the absence of AMPARs

In 0 mM Mg^{2+} ACSF, bath application of NBQX at increasing concentrations decreased ∫XIIn amplitude ($EC_{50} = 0.1$ μM, $n = 4$), decreased I_I peak recorded from neurons voltage-clamped at -60 mV ($EC_{50} = 0.001$ μM, $n = 4$, Fig. 4A and 5A) and did not significantly affect period until very high concentrations (≥ 100 μM, $EC_{50} = 64.7$ μM, Fig. 5B). There was a 500-fold increase in the NBQX EC_{50} for period with respect to the EC_{50} in control ACSF. Thus, in 0 mM Mg^{2+} ACSF, ∫XIIn discharges and I_I were measurable at NBQX concentrations that abolished I_I in control ACSF. Concentrations as high as 100 μM of NBQX were unable to block either I_I or rhythmic XIIn activity ($n = 4$, Figs 4A and 5A). To test whether after blockade of AMPARs the remaining I_I was attributable to active NMDARs, we simultaneously bath-applied MK-801 (20 μM) along with increasing concentrations of NBQX (0.01–0.5 μM). In the presence of MK-801, lower concentrations of NBQX produced

the same decrease in $\int$XIIn amplitude ($EC_{50} = 0.18\ \mu M$, $n = 4$, Fig. 4B) and in I_I peak at -60 mV ($EC_{50} = 0.1\ \mu M$, $n = 4$, Figs 4B and 5A), as well as the same increase in period ($EC_{50} = 0.12\ \mu M$, Fig. 5B). In the presence of MK-801, 0.5 μM NBQX abolished I_I, and thus XIIn activity (Figs 4B and 5A).

Analysis of Q_I in 0 mm Mg^{2+} unmasks several components

Under control conditions AMPARs are the main carriers of Q_I with a small contribution of NMDARs. To quantify the contribution of NMDARs, we computed Q_I in the steady state of several experimental conditions and normalized those values against Q_I under control conditions ($Q_{I,ctrl} = 1$, Fig. 5C). Bath application of MK-801 reduced Q_I to 0.89 ± 0.07, meaning that $Q_{I,NMDAR} = 0.11$. In 0 mm Mg^{2+}, Q_I increased to 4.09 ± 0.5. We assumed that

removal of the voltage-dependent Mg^{2+} blockade activated NMDARs that were silent under control conditions. Further bath application of MK-801 eliminated the NMDAR-mediated fraction ($Q_{I,total,NMDAR}$), reducing Q_I to 2.78 ± 0.6, still substantially larger than $Q_{I,ctrl}$. We assumed that this anomalous increase in Q_I is attributable to non-specific effects of Mg^{2+} removal, such as an increase of neurotransmitter release from presynaptic terminals, increasing AMPAR- and other neurotransmitter receptor-mediated currents. In 0 mm Mg^{2+} and 50 μM NBQX, Q_I was 2.07 ± 0.34. We assume that, in this case NBQX blocked $Q_{I,AMPAR}$ and a fraction of $Q_{I,non\text{-}specific}$ mediated by AMPAR, then the Q_I carriers were $Q_{I,total,NMDAR}$ and $Q_{I,non\text{-}specific,non\text{-}AMPAR}$.

In summary, in standard conditions AMPARs are the main carriers of Q_I, with a small contribution of NMDARs. A large fraction of NMDARs do not pass current due to the Mg^{2+} block. In the absence of Mg^{2+} that large fraction
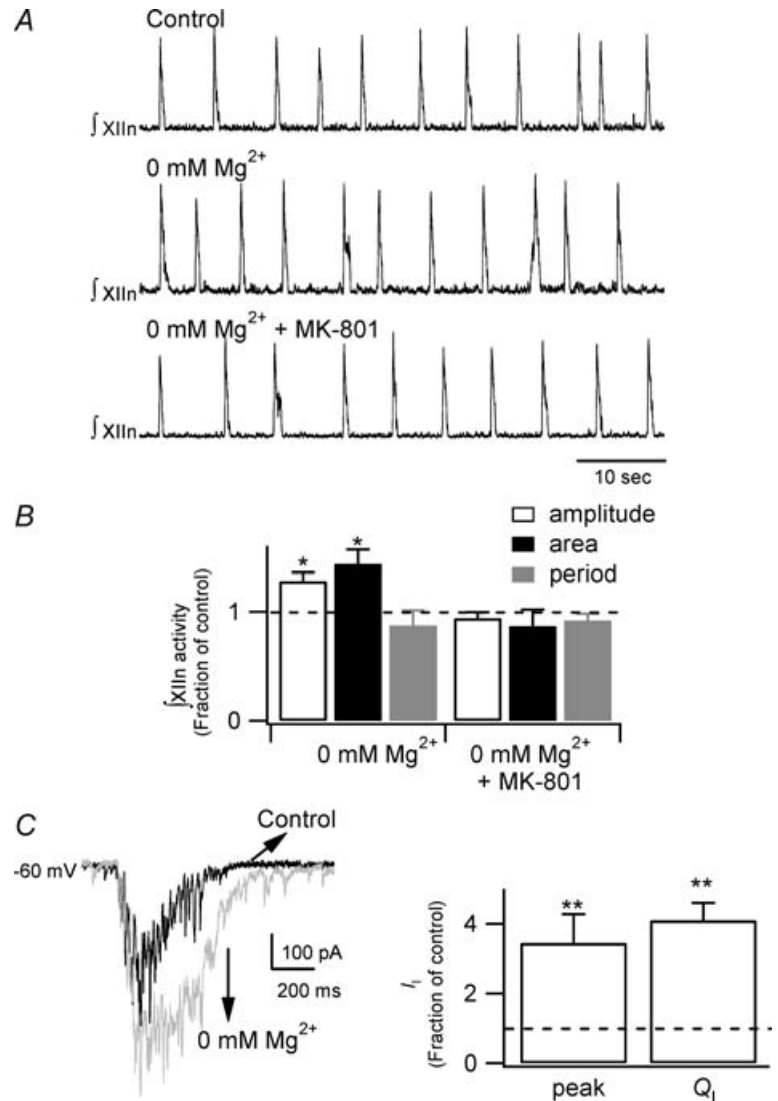
Figure 3. Endogenous NMDAR activation affects $\int$XIIn amplitude and area, I_I and Q_I, but not period
A and B, perfusion of slices with 0 mm Mg^{2+} ACSF increased $\int$XIIn amplitude and area 28% and 43%, respectively, with respect to basal rhythmic activity (Control). $\int$XIIn period in control conditions was 6.3 ± 1.2 s ($n = 4$) and in 0 mm Mg^{2+} ACSF was 5.5 ± 0.7 s. Bath application of MK-801 brought $\int$XIIn amplitude, area and period values back to control. $\int$XIIn period in this condition was 5.8 ± 0.3 s. C, in preBötC neurons voltage-clamped at -60 mV and perfused with 0 mm Mg^{2+} ACSF, I_I peak and Q_I increased 245% and 309%, respectively, with respect to I_I in control conditions. Representative traces: black: control; grey: 0 mm Mg^{2+}. (*$P < 0.05$; **$P < 0.01$.)

of NMDARs is unmasked and, in the presence of NBQX, became the major Q_I carrier.

NMDARs drive the respiratory rhythm in 3 mm K$^+$

Our slices exhibit a robust rhythm in 9 mm K$^+$ and are silent in 3 mm K$^+$ ACSF under standard conditions (data not shown). We questioned whether the additional I_I generated by NMDARs in the absence of Mg^{2+} would be enough to drive the respiratory rhythm in 3 mm K$^+$. After recording activity in control ACSF (with 9 mm K$^+$ and 1.5 mm Mg^{2+}), we washed in a test ACSF with 3 mm K$^+$ and 0 mm Mg^{2+}. This increased I_I peak and Q_I in preBötC neurons voltage-clamped at -60 mV by 100% ($P < 0.05$, $n = 6$, Fig. 6C) and by 170% ($P < 0.05$), respectively, and increased $\int$XIIn amplitude and area by 30% ($P < 0.01$, $n = 6$) and 34% ($P < 0.05$), respectively. Under control conditions, the period was 5.5 ± 1.26 s ($n = 6$); test ACSF increased the period to 13.6 ± 1.06 s ($P < 0.05$, $n = 6$).

Bath replacement with 3 mm K$^+$, 1.5 mm Mg^{2+} ACSF ($n = 3$, Fig. 6A) or bath application of MK-801 ($n = 3$, Fig. 6B) completely abolished I_I and rhythmic XIIn activity.

Discussion

Under control conditions in respiratory rhythmic slices from neonatal rats, NMDARs in preBötC neurons appear activated during inspiration but do not pass significant amounts of current due to their voltage-dependent block. However, NMDARs can significantly contribute to or even solely drive the respiratory rhythm in these slices in situations where the voltage-dependent block is substantially attenuated.

NMDARs are not required for prenatal development of respiratory networks (Funk *et al.* 1997). In medullary slice or *en bloc* brainstem–spinal cord preparations from neonatal rodents under baseline conditions, NMDARs are not required for generation of respiratory rhythm or motor output, yet exogenous application of NMDA produces a robust response (Greer *et al.* 1991; Funk *et al.* 1993, 1997). Furthermore, removal of extracellular Mg^{2+} enhances inspiratory currents in preBötC neurons, suggesting that endogenous NMDAR activation can enhance the discharge normally due to currents through AMPARs (Pierrefiche *et al.* 1991).

We suggest that during each inspiratory cycle only a small fraction of preBötC neuron NMDARs are sufficiently depolarized to remove the Mg^{2+} block. How big a depolarization is needed to remove the Mg^{2+} block? That depends on NMDAR subunit composition. NR1/2A (composed of NR1 and NR2A subunits) and NR1/2B receptors are more strongly inhibited at hyperpolarized potentials by Mg^{2+} than NR1/2C or NR1/2D receptors (Kuner & Schoepfer, 1996). In recombinant systems, inclusion of NR3A with NR1 and NR2 in heteromultimeric channels reduces the sensitivity to Mg^{2+} block and
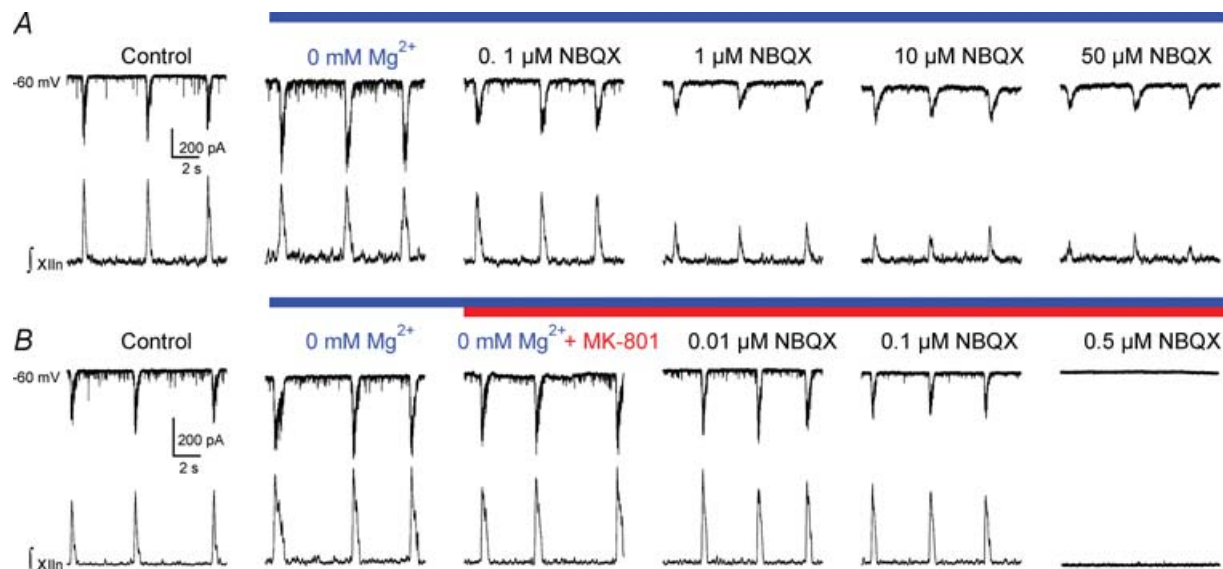
Figure 4. NMDARs drive the respiratory rhythm in the absence of AMPARs
In 0 mm Mg^{2+} ACSF, $\int$XIIn discharges and I_I from preBötC neurons were measurable at NBQX concentrations in which I_I was no longer measurable in basal conditions. *A*, bath application of NBQX at increasing concentrations decreased the $\int$XIIn amplitude but did not affect period. Concentrations as high as 100 μM of NBQX were unable to block either the I_I in preBötC neurons or the $\int$XIIn activity ($n = 4$). I_I peak remained virtually unchanged in 1–100 μM NBQX. *B*, in the presence of MK-801, lower concentrations of NBQX were necessary to decrease $\int$XIIn amplitude and I_I peak, as well as to increase period. NBQX at 0.5–1 μM abolished I_I.
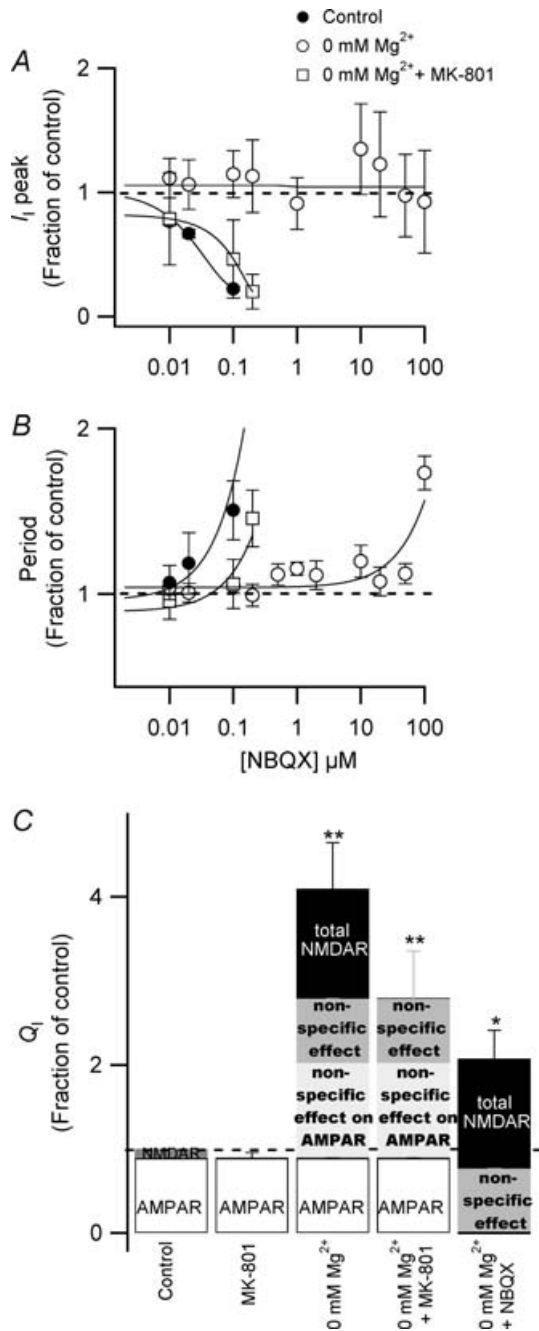
Figure 5. In 0 mm Mg^{2+} MK-801 shifted the NBQX dose–response curves for I_I and period to values similar to those in the presence of Mg^{2+}

A, in 0 mm Mg^{2+} (○) bath application of NBQX at increasing concentrations decreased the I_I peak recorded from neurons voltage-clamped at −60 mV (EC$_{50}$ = 0.001 μM, $n = 4$, note that in the absence of NBQX, 0 mm Mg^{2+} increased I_I 3.4 ± 0.8 times with respect to control). I_I from preBötC neurons was measurable at NBQX concentrations in which I_I was no longer measurable in control conditions (●). In the absence of Mg^{2+} and the presence of MK-801 (□), lower concentrations of NBQX were necessary to decrease I_I peak at −60 mV (EC$_{50}$ = 0.1 μM, $n = 4$). NBQX dose–response curve for I_I peak in the presence of MK-801 is similar to the curve in control conditions (EC$_{50}$ = 0.02 μM, $n = 4$). *B*, in 0 mm Mg^{2+} bath application

results in a smaller unitary conductance than NR1/NR2 channels. Consistent with that, in NR3A-deficient mice, NMDA-evoked currents of cortical neurons are larger than in wild-type littermates (Das *et al.* 1998; Sasaki *et al.* 2002).

Single-cell RT-PCR analysis reveals that NR2A, NR2B and NR2D are expressed in similar amounts in preBötC neurons, XII motoneurons and neurons from the nucleus of the solitary tract (NTS) in young rats, whereas NR3A is expressed in all preBötC neurons but only in one-third of XII motoneurons and NTS neurons (Paarmann *et al.* 2005). We suggest that under control conditions, the depolarization achieved during the initial phase of each inspiratory burst relieves the Mg^{2+} block of NR3A-containing receptors, which are less sensitive to the voltage-dependent blockade. Since these receptors have a small unitary conductance, their contribution to Q_I is not significant. Depolarizing a neuron or removing the extracellular Mg^{2+} unmasks the fraction of NMDARs that under control conditions are presumably active, i.e. bound by glutamate, but not passing current. This fraction must contain NR1/NR2A and NR1/NR2B receptors that are strongly blocked near resting membrane potentials by Mg^{2+} at physiological concentrations.

An interesting observation is that inhibition of glutamate uptake enhances both the AMPAR- and the NMDAR-mediated components of I_{Glu} in preBötC neurons voltage-clamped at −60 mV. We suggest that increased glutamate accumulation in the synapse increases the AMPAR-mediated depolarization of preBötC neurons sufficiently to remove the voltage-dependent block of NMDARs (MacDonald & Nowak, 1990) allowing them to pass current.

In the absence of Mg^{2+}, NBQX concentrations higher than 1 μM decreased ∫XIIn amplitude while I_I peak and period remain virtually unchanged. We suggest that the AMPAR/NMDAR ratio is higher in XIIn motoneurons than in preBötC neurons, making them more sensitive to AMPA blockade.

Though in standard control conditions NMDARs are not the major charge carrier for I_I, the Ca^{2+} influx they provide could contribute to activation of much larger inward currents such as the Ca^{2+}-activated mixed cationic current (I_{CAN}) that is present in all preBötC neurons and are hypothesized to be an important intrinsic burst-generating current (Rekling & Feldman, 1998; Pena *et al.* 2004; Del Negro *et al.* 2005).

of NBQX at increasing concentrations increased period (EC$_{50}$ = 64.65 μM). The EC$_{50}$ for period was 500 times greater with respect to the EC$_{50}$ in control conditions (EC$_{50}$ = 0.13 μM). Bath application of MK-801 increased period to values close to control conditions (EC$_{50}$ = 0.12 μM). *C*, analysis of synaptic charge (Q_I) reveals the contribution of different components. Values were normalized against control (Q_{I_ctrl} = 1). See Results for description. (*$P < 0.05$; **$P < 0.01$.)

Implications for respiratory rhythm generation

The group-pacemaker hypothesis posits that preBötC inspiratory neurons mutually interconnected by glutamatergic synapses initiate inspiration by generating a population burst of activity arising from a recurrent network with positive feedback (Rekling & Feldman, 1998). Here we show that, in the absence of AMPAR-mediated synaptic transmission, NMDARs can provide the excitatory drive necessary to initiate and propagate the inspiratory burst. Under our experimental conditions, NMDARs in preBötC neurons can replace AMPARs in mediating excitatory interactions since: (i) Both receptors are coexpressed in preBötC neurons (at present we do not know if they have similar somatodendritic or synaptic distribution; Paarmann *et al.* 2000); (ii) NMDAR current slope in the absence of

Mg^{2+} is similar to that of AMPARs; and (iii) NMDAR activation can recruit a set of intrinsic conductances resembling those activated by AMPARs, and also induce pacemaker-like membrane potential oscillations (Grillner & Wallen, 1985). These currents are not identical, however. A striking difference is that NMDARs are permeable to Ca^{2+} whereas in preBötC neurons, AMPARs almost exclusively contain R-edited GluR2 (Paarmann *et al.* 2000) and are mainly permeable to Na^+ (authors' unpublished observations) but not Ca^{2+}. This would suggest that Ca^{2+} entry through synaptic receptors is not playing a critical role in rhythmogenesis, which is of considerable interest because the Ca^{2+} buffering of these neurons appears to be limited (Alheid *et al.* 2002). We suggest that the major source of Ca^{2+} entry in preBötC neurons is through voltage-gated Ca^{2+} channels activated
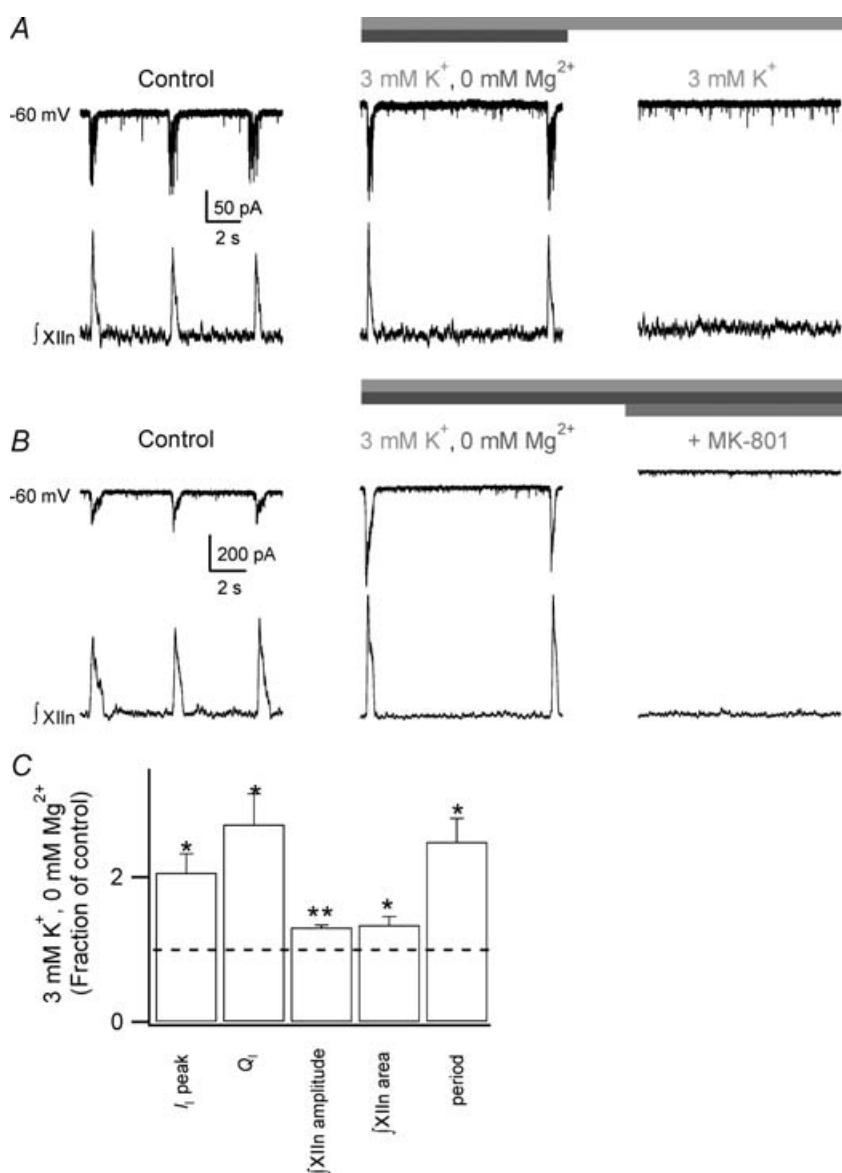
Figure 6. NMDARs drive the respiratory rhythm in 3 mm K$^+$

A, I_l and ∫XIIn discharges from a preBötC neuron voltage-clamped at −60 mV in standard conditions. Lowering the extracellular [K$^+$] to 3 mm in 0 mm Mg^{2+} ACSF increased the peak I_l but slowed the rhythm. Increasing the [Mg^{2+}] to basal values abolished the rhythm. *B*, same as in *A*. In 3 mm K$^+$, 0 mm Mg^{2+} ACSF, bath application of MK-801 abolished the rhythm. *C*, summary of the effects of lowering extracellular [K$^+$] to 3 mm in the absence of Mg^{2+}. (*P < 0.05; **P < 0.01.)

during action potentials (C. Morgado-Valle and J. L. Feldman, unpublished data).

Removal of extracellular Mg^{2+} increased the I_I and the $\int$XIIn amplitude but slightly decreased the period. In contrast, lowering the ACSF $[K^+]$ to 3 mM in the absence of Mg^{2+} increased the I_I and $\int$XIIn amplitude but almost tripled the period. Thus, an increase in I_I does not necessarily result in an increase in frequency. This would suggest that I_I affects the amplitude of the motor output whereas frequency depends on the level of excitability of preBötC neurons.

Clinical relevance

Our findings may have clinical relevance. Patients with hyperventilation syndrome (HVS), a breathing pattern disorder characterized by bouts of inappropriately high ventilation associate with elevated frequency, often have significant hypomagnesaemia (Fehlinger & Seidel, 1985; Durlach et al. 1997). Patients with Rett's syndrome also have frequent episodes of hyperventilation; supplemental dietary Mg^{2+} ameliorates these episodes (Egger et al. 1992). Our work suggests a potential causal link since decreased levels of Mg^{2+} could increase respiratory output (inappropriately) that is driven by the preBötC by mechanisms described above.

In summary, NMDARs are not necessary for respiratory rhythmogenesis under standard in vitro conditions. However, they can, after removing their voltage-dependent block due to Mg^{2+}, substitute for AMPAR-mediated glutamatergic transmission normally underlying respiratory pattern generation (at least in our experimental conditions). Moreover since I_I can be modulated independent of frequency and recurrent excitation is necessary for rhythm generation, network connectivity is an essential element underlying respiratory rhythmogenesis. Since Mg^{2+} levels can affect neuronal plasticity (Slutsky et al. 2004), an additional role of Mg^{2+} in breathing could be to modulate respiratory plasticity (Feldman et al. 2003), essential for adaptation of breathing to changing demands.

References

Alheid GF, Gray PA, Jiang MC, Feldman JL & McCrimmon DR (2002). Parvalbumin in respiratory neurons of the ventrolateral medulla of the adult rat. J Neurocytol 31, 693–717.

Anderson MK & Speck DF (1999). Differential effects of excitatory amino acid receptor antagonism in the ventral respiratory group. Brain Res 829, 69–76.

Chitravanshi VC & Sapru HN (1996). NMDA as well as non-NMDA receptors mediate the neurotransmission of inspiratory drive to phrenic motoneurons in the adult rat. Brain Res 715, 104–112.

Connelly CA, Otto-Smith MR & Feldman JL (1992). Blockade of NMDA receptor- channels by MK-801 alters breathing in adult rats. Brain Res 596, 99–110.

Das S, Sasaki YF, Rothe T, Premkumar LS, Takasu M, Crandall JE, Dikkes P, Conner DA, Rayudu PV, Cheung W, Chen HS, Lipton SA & Nakanishi N (1998). Increased NMDA current and spine density in mice lacking the NMDA receptor subunit NR3A. Nature 393, 377–381.

Del Negro CA, Morgado-Valle C, Hayes JA, Mackay DD, Pace RW, Crowder EA & Feldman JL (2005). Sodium and calcium current-mediated pacemaker neurons and respiratory rhythm generation. J Neurosci 25, 446–453.

Durlach J, Bac P, Durlach V, Bara M & Guiet-Bara A (1997). Neurotic, neuromuscular and autonomic nervous form of magnesium imbalance. Magnes Res 10, 169–195.

Egger J, Hofacker N, Schiel W & Holthausen H (1992). Magnesium for hyperventilation in Rett's syndrome. Lancet 340, 621–622.

Fehlinger R & Seidel K (1985). The hyperventilation syndrome: a neurosis or a manifestation of magnesium imbalance? Magnesium 4, 129–136.

Feldman JL, Mitchell GS & Nattie EE (2003). Breathing: rhythmicity, plasticity, chemosensitivity. Annu Rev Neurosci 26, 239–266.

Feldman JL, Windhorst U, Anders K & Richter DW (1992). Synaptic interaction between medullary respiratory neurones during apneusis induced by NMDA-receptor blockade in cat. J Physiol 450, 303–323.

Foutz AS, Champagnat J & Denavit-Saubie M (1988). N-methyl-D-aspartate (NMDA) receptors control respiratory off-switch in cat. Neurosci Lett 87, 221–226.

Foutz AS, Champagnat J & Denavit-Saubie M (1989). Involvement of N-methyl-D-aspartate (NMDA) receptors in respiratory rhythmogenesis. Brain Res 500, 199–208.

Funk GD, Johnson SM, Smith JC, Dong XW, Lai J & Feldman JL (1997). Functional respiratory rhythm generating networks in neonatal mice lacking NMDAR1 gene. J Neurophysiol 78, 1414–1420.

Funk GD, Smith JC & Feldman JL (1993). Generation and transmission of respiratory oscillations in medullary slices: role of excitatory amino acids. J Neurophysiol 70, 1497–1515.

Greer JJ, Smith JC & Feldman JL (1991). Role of excitatory amino acids in the generation and transmission of respiratory drive in neonatal rat. J Physiol 437, 727–749.

Grillner S & Wallen P (1985). The ionic mechanisms underlying N-methyl-D-aspartate receptor-induced, tetrodotoxin-resistant membrane potential oscillations in lamprey neurons active during locomotion. Neurosci Lett 60, 289–294.

Kuner T & Schoepfer R (1996). Multiple structural elements determine subunit specificity of Mg^{2+} block in NMDA receptor channels. J Neurosci 16, 3549–3558.

MacDonald JF & Nowak LM (1990). Mechanism of blockade of excitatory amino acid receptor channels. Trends Pharmacol Sci 11, 167–172.

Paarmann I, Frrermann D, Keller BU & Hollmann M (2000). Expression of 15 glutamate receptor subunits and various splice variants in tissue slices and single neurons of brainstem nuclei and potential functional implications. J Neurochem 74, 1335–1345.

Paarmann I, Frermann D, Keller BU, Villmann C, Breitinger HG & Hollmann M (2005). Kinetics and subunit composition of NMDA receptors in respiratory-related neurons. *J Neurochem* **93**, 812–824.

Pena F, Parkis MA, Tryba AK & Ramirez JM (2004). Differential contributions of pacemaker properties to the generation of respiratory rhythms during normoxia and hypoxia. *Neuron* **43**, 105–117.

Pierrefiche O, Schmid K, Foutz AS & Denavit-Saubie M (1991). Endogenous activation of NMDA and non-NMDA glutamate receptors on respiratory neurones in cat medulla. *Neuropharmacology* **30**, 429–440.

Rekling JC & Feldman JL (1998). PreBötzinger complex and pacemaker neurons: hypothesized site and kernel for respiratory rhythm generation. *Annu Rev Physiol* **60**, 385–405.

Rothman S (1988). Noncompetitive N-Methyl-D-aspartate antagonist affect multiple ionic currents. *J Pharmacol Exp Ther* **246**, 137–142.

Sasaki YF, Rothe T, Premkumar LS, Das S, Cui J, Talantova MV, Wong HK, Gong X, Chan SF, Zhang D, Nakanishi N, Sucher NJ & Lipton SA (2002). Characterization and comparison of the NR3A subunit of the NMDA receptor in recombinant systems and primary cortical neurons. *J Neurophysiol* **87**, 2052–2063.

Slutsky I, Sadeghpour S, Li B & Liu G (2004). Enhancement of synaptic plasticity through chronically reduced Ca^{2+} flux during uncorrelated activity. *Neuron* **44**, 835–849.

Smith JC, Ellenberger HH, Ballanyi K, Richter DW & Feldman JL (1991). Pre-Bötzinger complex: a brainstem region that may generate respiratory rhythm in mammals. *Science* **254**, 726–729.

Wooltorton JR & Mathie A (1995). Potent block of potassium currents in rat isolated sympathic neurons by the uncharged from of amitriptyline and related tricyclic compounds. *Br J Pharmacol* **116**, 2191–2200.